Persistent current-carrying state of charge quasiparticles in an *np* ribbon featuring a single Dirac cone

Anatoly M. Kadigrobov and Ilya M. Eremin
Institut für Theoretische Physik III, Ruhr-Universität Bochum, D-44801 Bochum, Germany

(Received 27 April 2023; accepted 22 September 2023; published 9 October 2023)

The formation of persistent charge currents in mesoscopic systems remains an interesting and actual topic of condensed matter research. Here, we analyze the formation of spontaneous arising persistent currents of charged fermions in two-dimensional electron-hole ribbons on the top and bottom of a three-dimensional topological insulator. In such a device the two-dimensional Dirac fermions with opposite chiralities are spatially separated, which allows these currents to flow in the opposite directions without compensating each other. The nature of this phenomenon is based on the interference of the quasiparticle quantum waves that are scattered with asymmetric scattering phases at the lateral *np* chiral junction and then reflected back by the external boundaries of the ribbon. As a result, quasiparticles in the ribbon are shown to be in unified electron-hole quantum states carrying the persistent current.

DOI: 10.1103/PhysRevB.108.155407

I. INTRODUCTION

The formation of persistent currents in solid state systems has always been a subject of intense debate. Initially Felix Bloch demonstrated the impossibility of persistent electric currents in the ground many-body state of interacting nonrelativistic systems, known currently as a Bloch theorem [1,2]. This theorem has been further extended to various cases of nonrelativistic systems [3–6]. Interestingly enough, the idea of spontaneous currents was also actively discussed in the context of the chiral magnetic [7–10] and vortical [11–13] effects. This yields an extension of the Bloch theorem to the relativistic systems, where it was shown that the chiral magnetic effect can be understood as a generalization of the Bloch theorem to a nonequilibrium steady state and the persistent axial currents are not prohibited [14].

At the same time, a persistent current state with zero resistance was theoretically predicted to exist in the system having an additional conserved charge [15,16]. Furthermore, for the mesoscopic systems, the persistent currents are not prohibited by the Bloch theorem and is of continuous interest for the community [17–24].

In this paper we analyze the formation of the persistent current carrying state in an *n*-*p* heterostructure made out of topological insulators, featuring an odd number of two-dimensional Dirac fermions (schematically shown in Fig. 1). Such mesoscopic devices with spatially separated Dirac fermion dispersions have been recently fabricated by various groups [25–30]. Here, we show that such a mesoscopic structure can host the persistent charge current carrying state. In particular, the device we anticipate consists of two tubes of three-dimensional topological insulators with an electron-hole asymmetry of the surface Dirac fermions on the surface due to the applied gate voltage. Then the two rings on the upper surface form an electron-hole junction (*np* junction), which is schematically shown in Fig. 1. The thicknesses W_e and W_h of the electron and hole rings, respectively, are assumed to satisfy the inequalities $W_e \sim W_h \gg \lambda_F$ where $\lambda_F = \hbar v/\varepsilon_F$ is the quasiparticle Fermi wave length while ε_F and v are their Fermi energy and the corresponding velocity. An important feature is that the Dirac cone in each side of the *np* junction is nondegenerate, which makes the topological insulator surface an ideal candidate for this junction.

II. THEORY

The quantum dynamics of quasiparticles (electrons and holes) on the surface of a topological insulator with a lateral electron-hole junction (*np* junction) is described by the two-component envelope wave function $\check{\psi}$ satisfying the Dirac equation

$$[V(y)-\varepsilon]\psi_1 + v\left(p_x - \hbar\frac{d}{dy}\right)\psi_2 = 0;$$
$$v\left(p_x + \hbar\frac{d}{dy}\right)\psi_1 + [V(y)-\varepsilon]\psi_2 = 0, \qquad (1)$$

where $V(y)$ is the lateral gate voltage potential extended along the x direction. Here, the axis x is parallel to the sample external boundaries and the *np* junction while the y axis is perpendicular to those as shown in Fig. 1.

Observe that Eq. (1) is itself symmetric with respect to the substitution of $p_x \to -p_x$. Indeed, there exists a unitary transformation matrix $U = \sigma_y$, $U^\dagger = \sigma_y$ that transforms $H(p_x, e)$ into $H(-p_x, e)$, which would imply $E(-p_x) = E(p_x)$. In what follows we show that the boundary conditions at the external ribbon edges as well as the condition of the electron and hole wave functions coupling at the *np* junction change the situation.

Note that the boundary conditions at external sharp lattice edges for the above equation were considered in various papers (see, e.g., review paper [31], and references therein). Here we use those, derived in Ref. [32], with the usage of the

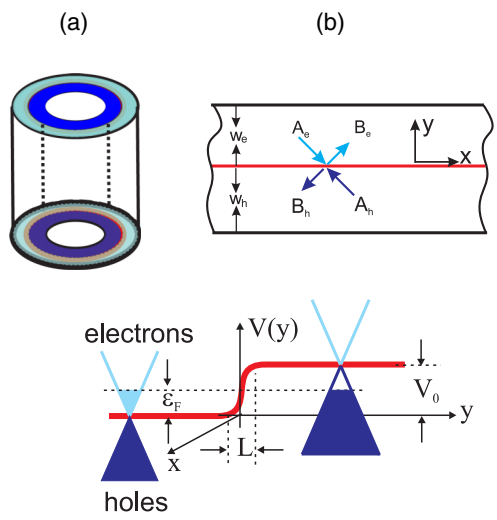

FIG. 1. Schematic presentation of the proposed np junction. Panel (a) shows the proposed experimental geometry, consisting of two hollow cylinders (tubes) of finite length embedded in each other, made of a topological insulator. (b) The thicknesses of the tubes are W_h and W_e, respectively, and the surface Dirac fermions form on the top and the bottom rings of the tube. The length of the tube is chosen such that one could ignore the interaction of Dirac surface bands from the upper and lower rings of the tube. Due to the applied gate voltage, the surface Dirac fermions on the upper surface of the inner and outer cylinders are differently doped, forming an np junction. (b) also shows thetwo-channel scattering of quasiparticles at the np junction on the top surface: Incident electron and hole waves with amplitudes A_e and A_h, respectively, tunnel through and are reflected back with amplitudes B_e and B_h (the tunneling is the interband one that transforms the electron into a hole and vice versa).

$\boldsymbol{k}\cdot\boldsymbol{p}$ approximation [33] and the analytical properties of the Green's functions of the Schrödinger equations (this derivation is briefly presented in Appendix).

In particular, the Dirac wave function is shown [32] to be a superposition of the virtual Bloch states belonging to different momenta and bands at the distances l from the sample sharp edge which are less than or of the same order as the atomic spacing a, $l \lesssim a$, while at $l \gg a$ all the virtual states exponentially drop out from the superposition and the wave function reduces to the difference between the incident and the reflected Kohn-Lattinger Bloch functions [33] of the topological insulator surface sheet. Hence, the boundary conditions for the Dirac equation in the vicinity of the ribbon edges $a \ll W_{e,h} - |y|$ can be written as follows:

$$\check{\psi}(p_x, y) = C[\check{\psi}^{(\mathrm{in})}(p_x, y) - \check{\psi}^{(\mathrm{out})}(p_x, y)], \tag{2}$$

where C is a constant and $\check{\psi}^{(\mathrm{in,out})}(p_x, y)$ are solutions of Eq. (1) for quasiparticle waves incoming and outgoing from the external boundaries (see Appendix).

In order to find the exact form of the boundary condition at the np junction we assume that the characteristic change interval L of the gate voltage $V(y)$ satisfies the condition $a \ll L \ll \lambda_F$ that allows one to use Eq. (1) in which $V(y)$ is approximated by the step function of the height V_0 (see Fig. 1):

$$V(y) = \begin{cases} 0, & y \leqslant 0 \\ V_0, & y \geqslant 0. \end{cases} \tag{3}$$

The general form of the solution of Eq. (1) can be expressed for holes ($y \geqslant 0$),

$$\check{\Psi}_h = A_h \frac{\sqrt{V_0-\varepsilon}}{v\sqrt{2p_h}} \begin{pmatrix} 1 \\ -\frac{v(p_x+ip_h)}{V_0-\varepsilon} \end{pmatrix} e^{iyp_h} + B_h \frac{\sqrt{V_0-\varepsilon}}{v\sqrt{2p_h}} \begin{pmatrix} 1 \\ -\frac{v(p_x-ip_h)}{V_0-\varepsilon} \end{pmatrix} e^{-iyp_h}, \tag{4}$$

and the electrons ($y \leqslant 0$),

$$\check{\Psi}_e = A_e \frac{\sqrt{\varepsilon}}{v\sqrt{2p_e}} \begin{pmatrix} 1 \\ \frac{v(p_x+ip_e)}{\varepsilon} \end{pmatrix} e^{iyp_e} + B_e \frac{\sqrt{\varepsilon}}{v\sqrt{2p_e}} \begin{pmatrix} 1 \\ \frac{v(p_x-ip_e)}{\varepsilon} \end{pmatrix} e^{-iyp_e}, \tag{5}$$

where $A_{e,h}$ and $B_{e,h}$ are the constants and

$$p_e = \sqrt{\left(\frac{\varepsilon}{v}\right)^2 - p_x^2}; \quad p_h = \sqrt{\left(\frac{V_0-\varepsilon}{v}\right)^2 - p_x^2}. \tag{6}$$

To find the constants, we match the electron and the hole wave functions at the interface of the np junction $y = 0$ and take into account the signs of the electron $v_y^{(e)} = v^2 p_y/\varepsilon$ and the hole velocity $v_y^{(h)} = -v^2 p_y/(V_0 - \varepsilon)$, respectively. The set of algebraic equations to determine the constants at the electron and hole wave function inside the region $\varepsilon \leqslant V_0/2$, $|p_x| \leqslant \varepsilon/v$ and $V_0/2 \leqslant \varepsilon \leqslant V_0/$, $|p_x| \leqslant (V_0 - \varepsilon)/v$ have the form

$$\begin{gathered} \bar{A}_h + \bar{B}_h = \bar{A}_e + \bar{B}_e; \\ \frac{p_x + ip_h}{\varepsilon - V_0}\bar{A}_h + \frac{p_x - ip_h}{\varepsilon}\bar{B}_h = \frac{p_x + ip_h}{V_0 - \varepsilon}\bar{A}_e + \frac{p_x - ip_h}{V_0 - \varepsilon}\bar{B}_e, \end{gathered} \tag{7}$$

where

$$\begin{aligned} \bar{A}_h &= \sqrt{\frac{V_0-\varepsilon}{2p_h}}A_h; \quad \bar{B}_h = \sqrt{\frac{V_0-\varepsilon}{2p_h}}B_h; \\ \bar{A}_e &= \sqrt{\frac{\varepsilon}{2p_e}}A_h; \quad \bar{B}_e = \sqrt{\frac{\varepsilon}{2p_e}}B_e. \end{aligned} \tag{8}$$

Outside of the above-mentioned area, $\varepsilon \leqslant V_0/2$, $(V_0 - \varepsilon)/v \geqslant |p_x| \geqslant \varepsilon/v$, and $\varepsilon \geqslant V_0/2$, $(V_0 - \varepsilon)/v \leqslant |p_x| \leqslant \varepsilon/v$, holes undergo the complete internal reflections at the np junction. For the hole momentum and the energy inside the indicated limits, one finds that the electron momentum projection p_y is imaginary, $p_y^{(e)} = i\sqrt{p_x^2 - (\varepsilon/v)^2}$, and hence the electron wave function (into which the incident hole is transformed after passing through the np junction) exponentially decays inside the electronic part of the ribbon, $y < 0$. Taking this into account, we find at the interface of the np junction, $y = 0$:

$$\begin{aligned} \bar{A}_h + \bar{B}_h &= B_e - \bar{A}_h\frac{p_x + ip_h}{V_0 - \varepsilon} - \bar{B}_h\frac{p_x - ip_h}{V_0 - \varepsilon} \\ &= \bar{B}_e\frac{p_x - ip_e}{\varepsilon}. \end{aligned} \tag{9}$$

Next, solving Eqs. (7) one finds the 2×2 unitary matrix $\hat{\rho}$ that connects the constant factors A_e, A_h at the incident and

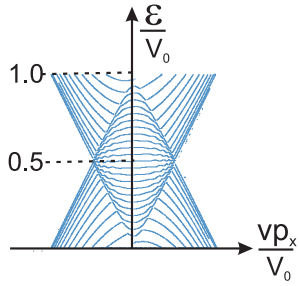

FIG. 2. Calculated spectrum of quasiparticles in the np ribbon, $\varepsilon_n(p_x)$. Numerical calculations are performed for the parameter $\Lambda = 50$. Inside the diamond [$\varepsilon \leqslant 0.5V_0$, $|p_x| \leqslant \varepsilon/v$ and $\varepsilon \geqslant 0.5V_0$, $|p_x| \leqslant (V_0 - \varepsilon)/v$] the spectrum corresponds to the unified electron-hole quantum interfering state, the energy bands being asymmetric, $\varepsilon_n(p_x) \neq \varepsilon_n(-p_x)$, and rather flat. Outside the diamond the spectrum is of the holes, $\varepsilon < 0.5V_0$, and electrons, $\varepsilon > 0.5V_0$ because the corresponding quasiparticles undergo total reflections at the np junction.

B_e, B_h at the outgoing wave functions [see also Fig. 1(b)]:

$$\hat{\rho} = e^{i\varphi}\begin{pmatrix} |r|e^{i\mu} & t \\ -t^{\star} & |r|e^{i\mu} \end{pmatrix}, \tag{10}$$

where

$$|r| = \left\{\frac{(V_0 p_x)^2 + [p_e(V_0 - \varepsilon) - p_h\varepsilon]^2}{(V_0 p_x)^2 + [p_e(V_0 + \varepsilon) + p_h\varepsilon]^2}\right\}^{1/2} \tag{11}$$

and

$$t = \frac{2\sqrt{p_e p_h \varepsilon(V_0 - \varepsilon)}}{\sqrt{(V_0 p_x)^2 + [p_e(V_0 - \varepsilon) + p_h\varepsilon]^2}} \tag{12}$$

are the probability amplitudes for an incident quasiparticle to be reflected back or to be transmitted through the barrier, respectively, while

$$\varphi = \pi + \arctan\frac{p_e(V_0 - \varepsilon) + p_h\varepsilon}{V_0 p_x} \tag{13}$$

and

$$\mu = \arctan\frac{p_e(V_0 - \varepsilon) - p_h\varepsilon}{V_0 p_x} \tag{14}$$

are the scattering phases. Most importantly, it follows from Eqs. (13) and (14) that scattering phases are asymmetric, i.e., $\varphi(p_x) \neq \varphi(-p_x)$, $\mu(p_x) \neq \mu(-p_x)$. This will be the origin of current-carrying state.

Note, the unitary scattering matrix $\hat{\rho}$ describes interband electron-hole tunneling that takes place inside the area defined by the following inequalities: $\varepsilon \leqslant V_0/2$, $|p_x| \leqslant \varepsilon/v$ and $V_0/2 \leqslant \varepsilon \leqslant V_0/$, $|p_x| \leqslant (V_0 - \varepsilon)/v$ which is seen as a diamond in Fig. 2. The boundaries of this area are defined by the condition that the transverse momenta p_e and p_h are real.

Matching the solutions of the Dirac equation, Eqs. (4) and (5), with the usage of the boundary condition at the sample edges, Eq. (2), and the scattering matrix at the np junction, Eq. (10), one finds the dispersion equation for the quasiparticles in the np ribbon as follows. (1) Inside the energy and momentum intervals $\varepsilon \leqslant V_0/2$, $|p_x| \leqslant \varepsilon/v$ and $\varepsilon \geqslant (V_0 - \varepsilon)/2$, $|p_x| \leqslant (V_0 - \varepsilon)/v$ the dispersion equation is

$$D(\varepsilon, p_x) \equiv \cos[\Phi_e - \Phi_h + \varphi] + |r|\cos[\Phi_e + \Phi_h + \mu] = 0, \tag{15}$$

where

$$\Phi_e(\varepsilon, p_x) = \frac{W_e p_e(\varepsilon, p_x)}{\hbar}; \quad \Phi_h(\varepsilon, p_x) = \frac{W_h p_h(\varepsilon, p_x)}{\hbar}. \tag{16}$$

(2) Outside the above-mentioned intervals the quasiparticles undergo the complete internal reflections at the np junction, Eq. (9), and their dispersion equations are

$$D_h(\varepsilon, p_x) = \sin[\Phi_h - \varphi_h]; \quad |p_x| \geqslant \frac{\varepsilon}{v}, \ \varepsilon \leqslant \frac{V_0}{2};$$
$$D_e(\varepsilon, p_x) = \sin[\Phi_e + \varphi_e]; \quad |p_x| \geqslant \frac{V_0 - \varepsilon}{v}, \ \varepsilon \geqslant \frac{V_0}{2}, \tag{17}$$

where

$$\varphi_h = \pi + \arctan\left[\frac{p_h\varepsilon}{V_0 p_x + |p_e|(V_0 - \varepsilon)}\right];$$
$$\varphi_e = \pi + \arctan\left[\frac{p_e(V_0 - \varepsilon)}{(V_0 p_x - |p_h|\varepsilon)}\right]. \tag{18}$$

Solutions of Eqs. (15)–(17) give the dispersion law of the electron-hole quasiparticles in the np ribbon, $\varepsilon_n(p_x)$, presented in Fig. 2. As follows from Eqs. (15) and (17), quasiparticles in the np ribbon are electron-hole coupled states only inside the diamond [$\varepsilon \leqslant 0.5V_0$, $|p_x| \leqslant \varepsilon/v$ and $\varepsilon \geqslant 0.5V_0$, $|p_x| \leqslant (V_0 - \varepsilon)/v$] shown in Fig. 2. Outside the diamond, $\varepsilon \leqslant 0.5V_0$, $|p_x| \geqslant \varepsilon/v$ and $\varepsilon \geqslant 0.5V_0$, $|p_x| \geqslant (V_0 - \varepsilon)/v$, electrons and holes undergo the complete internal reflections at the np junction and their dispersion equations are defined by Eq. (17). Inside the diamond, the spectrum consists of a series of extremely narrow bands of width $\Delta\varepsilon \sim 2\pi\hbar v/W$ and the dispersion depends on the variation of the momentum, $\Delta p_x \sim \hbar/W$. Such a peculiar spectrum is the result of the quantum interference of the electron and hole waves.

As this quantum interference is associated with the two-channel scattering of the waves at the np junction [which breaks the symmetry $p_x \to -p_x$ of the scattering phases; see Eq. (15) and Eqs. (13) and (14)], it results in the asymmetry of the new quasiparticle velocity $\bar{v}_x(\varepsilon, p_x) \neq \bar{v}_x(\varepsilon, -p_x)$ where

$$\bar{v}_x = \frac{d\varepsilon_n(p_x)}{dp_x} = -\frac{\partial D/\partial p_x}{\partial D/\partial\varepsilon}, \quad D(\varepsilon, p_x) = 0. \tag{19}$$

As one easily sees from Eqs. (15), (13), and (14) the dispersion equation $D(\varepsilon, p_x) = 0$ is asymmetric with respect to the momentum inversion, $p_x \to -p_x$, and hence the spectrum of electron-hole quasiparticles is asymmetric as well, $\varepsilon_n(p_x) \neq \varepsilon_n(-p_x)$. Therefore, velocities $v_x(p_x) \neq v_x(-p_x)$ and quasiparticles with opposite directions of p_x momenta carry the probability density currents of unequal magnitudes. As a result, the quantum ground state of the electron-hole Fermi gas in the np ribbon or a ring carries a persistent current in the absence of any external fields, which is a rather remarkable result.

It is worthy to note that the phenomenon under consideration is absent in an electron or hole graphene ribbon in which the electron-hole interference is absent. In this case the corresponding dispersion laws are symmetric and the probability

currents flowing in the opposite directions compensate each other. Note, in contrast to the conventional persistent current under magnetic field the predicted phenomenon is based on the combination of the quantum interference which arises after two-channel scattering of the quasiparticle waves at the np junction and then reflected back by the external ribbon boundaries, and the asymmetry of the scattering phases with respect to $p_x \to -p_x$ [see Eqs. (13) and (14)]. This also puts a constraint on the observability of the effect, which requires a mesoscopic size of the junction and its good transparency.

An expression for the peculiar persistent current under consideration can be obtained in the following form:

$$j_{ps} = -2e\,\mathrm{Tr}[\hat{v}_x f_0(\hat{H})] = -\frac{e}{\pi\hbar}\int d\varepsilon\, f_0[\varepsilon]\int dp_x \bar{v}_x[\varepsilon, p_x]\sum_n \delta[\varepsilon - \varepsilon_n(p_x)]. \tag{20}$$

To calculate it we use the approach developed previously for magnetic breakdown systems [34]. Namely, using the identity

$$\sum_n \delta[\varepsilon - \varepsilon_n(p_x)] = \left|\frac{\partial D(\varepsilon, p_x)}{\partial \varepsilon}\right| \delta[D(\varepsilon, p_x)] \tag{21}$$

together with Eq. (19) one presents Eq. (20) in the following form:

$$j_{ps} = -\frac{e}{\pi\hbar}\int d\varepsilon\, f_0[\varepsilon]\int dp_x \frac{\partial D(\varepsilon, p_x)}{\partial p_x}\delta[D(\varepsilon, p_x)]. \tag{22}$$

As one sees from Eq. (6), $p_e(\varepsilon) \leqslant p_h(\varepsilon)$ if $\varepsilon \leqslant V_0/2$ and $p_h(\varepsilon) \leqslant p_e(\varepsilon)$ if $\varepsilon \geqslant V_0/2$. On the other hand, $D(\varepsilon, p_x)$ in the integrand of Eq. (22) has a jump $p_x = \pm 0$. Taking it into account one rewrites Eq. (22) as follows:

$$\frac{j_{ps}}{e/\pi\hbar} = -\int_0^\infty d\varepsilon\, f_0(\varepsilon)\{\Theta[D(\varepsilon, -0)] - \Theta[D(\varepsilon, +0)]\} + \int_0^{V_0/2} d\varepsilon\, f_0(\varepsilon)\left\{\int_{-p_h^{(m)}}^{-p_e^{(m)}} \frac{d\Theta[D_h]}{dp_x}dp_x + \int_{p_e^{(m)}}^{p_h^{(m)}} \frac{d\Theta[D_h]}{dp_x}dp_x\right\} + \int_{V_0/2}^{V_0} d\varepsilon f_0(\varepsilon)\{\cdots\}, \tag{23}$$

where

$$p_e^{(m)} = \frac{\varepsilon}{v}; \quad p_h^{(m)} = \frac{V_0 - \varepsilon}{v} \tag{24}$$

are the maximal electron and hole momenta, respectively, while according to Eqs. (13)–(15) one has

$$D(\varepsilon, \pm 0) = \cos\left[\frac{W(V_0 - 2\varepsilon)}{\hbar v} \mp \frac{\pi}{2}\right]. \tag{25}$$

Using the equalities $D(\varepsilon, p_e^{(m)}) = D_h(\varepsilon, p_e^{(m)})$ and $D_h(\varepsilon, -p_h^{(m)}) = D_h(\varepsilon, p_h^{(m)})$ valid at $\varepsilon \leqslant V_0/2$, and $D(\varepsilon, p_h^{(m)}) = D_e(\varepsilon, p_h^{(m)})$ and $D_e(\varepsilon, -p_e^{(m)}) = D_e(\varepsilon, p_e^{(m)})$ valid at $\varepsilon \geqslant V_0/2$ [see Eqs. (15) and (17)] one finds the final expression for the quantum interference persistent current

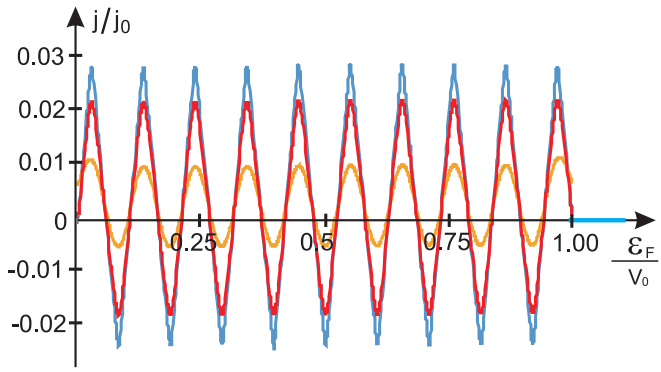

FIG. 3. Calculated dependence on ε_F/V_0 of the current j_{ps} flowing along the np ribbon in the absence of external fields. Numerical calculations are performed for $\Lambda = WV_0/\hbar v = 30$. Curves of the largest and smallest amplitudes (blue and orange. respectively) are at $T = 0$ and $T = 10^{-2}V_0$, respectively. The curve of the middle amplitude (red) is for a dirty graphene $W_e + W_h = 12l_0$ at $T = 0$ (l_0 is the quasiparticle free path length). The normalization parameter $j_0 = eV_0/\pi\hbar$ is of the order of the value of the current carried by the quasiparticles of the ribbon moving in the same direction.

flowing in the absence of external fields as follows:

$$\frac{j_{ps}}{j_0} = \int_0^1 f_0(z)\{\Theta[\sin[\Lambda(1-2z)]] - \Theta\{-\sin[\Lambda(1-2z)]\}\}dz, \tag{26}$$

where $\Theta(z)$ is the step function and

$$f_0(z) = \left(\exp\frac{(z - \varepsilon_F/V_0)}{T/V_0} + 1\right)^{-1}; \quad j_0 = \frac{eV_0}{\pi\hbar}; \ \Lambda = \frac{WV_0}{\hbar v}. \tag{27}$$

Here f_0 is the normalized Fermi distribution function, j_0 is the density of the current carried by the quasiparticles in the junction that has p_x momentum of the same sign; $\Lambda \gg 1$ is the semiclassical parameter. For the sake of simplicity, in what follows we consider $W_e = W_h = W$. The typical dependence of the current on the ratio between the Fermi energy and the gate voltage, ε_F/V_0, is presented in Fig. 3.

The integrand in the right-hand side of Eq. (26) comes from the jump of $D(\varepsilon, p_x)$ at $p_x = \pm 0$ [see Eqs. (13)–(15)]. The dependence of j_{ps} on ε_F/V_0 displays an oscillating character both in the current direction and in the amplitude, the latter being proportional to j_0/Λ. This decrease of the current amplitude by the semiclassical parameter $\Lambda \gg 1$ is determined by the fast semiclassical oscillations of the integrand in Eq. (26).

As the phenomenon under consideration is based on the asymmetry of the phases of the scattering amplitudes at the np junction, this persistent current has weak dependence on the scattering by impurities provided the latter (being symmetric) does not change the problem symmetry and hence the current. To show this we take into account the impurities by the simple broadening of the δ and Θ functions in Eqs. (20), (22), and (26) by $\gamma = \hbar v/l_0$ (the electron-impurity free path length is l_0) and the numerically calculated modified Eq. (26) for the ribbon width $W_e + W_h = 12l_0$ (see Fig. 3). In perfect analogy

to the conventional persistent current under magnetic field [35], the predicted current survives at distances $\lesssim l_\varphi$ at which the quasiparticle wave-function phase conserves.

The spontaneous current under consideration can flow along a closed np ribbon in the form of a ring formed on the top of the topological insulator cylinders, the radius of which satisfies the inequality $W \ll R \lesssim l_\varphi$ [see Figs. 1(a) and 1(b)]. In an np ribbon of length $l_{rib} \lesssim l_\varphi$ the spontaneous current is absent but there is a voltage drop between the ribbon ends, $V_r = j_{ps} l_{rib}/\sigma$, where σ is the conductivity of the ribbon. As follows from the above analysis, irradiation of the surface of the topological insulator top surface ring np ribbon excites the additional current predominantly flowing in one direction that may be used for the generation of a substantial photocurrent and the photovoltaic effect in single-cone Dirac systems (for investigations of the problems, see Refs. [36–38]).

III. CONCLUSION

To conclude, we analyze a peculiar persistent current formation along a mesoscopic electron-hole ribbon, formed on the surface of the topological insulator. Such currents may form even in the absence of both the magnetic and the electric fields and arise due to an odd number of Dirac cones, electron-hole asymmetry of the junction, and finite-size effects. We expect that in the case of the topological insulator [shown in Fig. 1 (a)] the Dirac fermions at the top and bottom of the sample have opposite chiralities and hence their persistent charge currents flow in opposite directions. Being spatially separated, these planar currents form the anti-Helmholtz coil (widely used for creating the cusp traps for ultracold atoms) producing an axially symmetric magnetic field in the form of the cusp around the middle of the coil axis. Therefore, the presence of the spontaneous persistent charge currents in such a topological insulator may be detected by measuring this specific magnetic field.

APPENDIX: DIRAC QUASIPARTICLE DYNAMICS AND BOUNDARY CONDITIONS

In this section the dynamics of quasiparticles and boundary conditions at the sharp lattice edge based on the $\boldsymbol{k}\cdot\boldsymbol{p}$ approximation is briefly described (their detailed analysis is presented in Ref. [32]).

Derivation of the boundary conditions is performed in two steps: (1) using the $\boldsymbol{k}\cdot\boldsymbol{p}$ approximation [33] (the Lattinger-Kohn model) one derives the Dirac equation for the envelope wave functions; (2) using the Green's functions for the Schrödinger equation expanded in terms of the Bloch functions of all bands and using the found connection between the Bloch functions and the envelope functions, one derives the boundary conditions sought for the envelope functions near the lattice sharp edge.

Step 1. The Schrödinger equation for noninteracting quasiparticles is written as

$$\left[-\frac{\hbar^2}{2m}\frac{\partial^2}{\partial \mathbf{r}^2} + U(\mathbf{r})\right]\varphi_{s,\mathbf{p}}(\mathbf{r}) = \varepsilon_s(\mathbf{p})\varphi_{s,\mathbf{p}}(\mathbf{r}), \tag{A1}$$

where $U(\mathbf{r}) = U(\mathbf{r}+\mathbf{a})$ is the lattice periodic potential ($\mathbf{a}$ is the lattice vector) and

$$\varphi_{s,\mathbf{p}}(\mathbf{r}) = e^{i(\mathbf{pr}/\hbar)}u_{s,\mathbf{p}}(\mathbf{r}) \tag{A2}$$

is the Bloch function while $u_{s,\mathbf{p}}(\mathbf{r})$ is its periodic factor, $\mathbf{p}$ is the electron quasimomentum while $\varepsilon_s(\mathbf{p})$ is the dispersion law, and $s = 1, 2$ are the band numbers of the electron and hole bands degenerated at $\mathbf{p} = 0$.

In the presence of a potential $V(\mathbf{r})$ the Schrödinger equation reads

$$\left[-\frac{\hbar^2}{2m}\frac{\partial^2}{\partial \mathbf{r}^2} + U(\mathbf{r}) + V(\mathbf{r})\right]\Psi(\mathbf{r}) = \varepsilon\Psi(\mathbf{r}). \tag{A3}$$

Here and below we assume that the potential $V(\mathbf{r})$ in a smooth function of the atomic scale.

To solve the problem we expand the wave function in terms of the modified Bloch functions (the Luttinger-Kohn functions)

$$\chi_{\alpha,\mathbf{p}} = \exp\left(i\frac{\mathbf{pr}}{\hbar}\right)u_{s,0}(\mathbf{r}) \tag{A4}$$

as follows:

$$\Psi(\mathbf{r}) = \sum_{s=1,2}\int g_{s,\mathbf{p}}\chi_{s,\mathbf{p}}(\mathbf{r})d\mathbf{p}. \tag{A5}$$

Using Eq. (A5) and the above-mentioned degeneration perturbation theory ("$\boldsymbol{k}\cdot\boldsymbol{p}$-method") one derives the Dirac equation (see Ref. [39] for details)

$$\begin{pmatrix} V(\mathbf{r}) & v\left(p_x - \hbar\frac{d}{dy}\right) \\ v\left(p_x + \hbar\frac{d}{dy}\right) & V(\mathbf{r}) \end{pmatrix}\begin{pmatrix}\psi_1\\ \psi_2\end{pmatrix} = \varepsilon\begin{pmatrix}\psi_1\\ \psi_2\end{pmatrix} \tag{A6}$$

for the envelope functions

$$\psi_{1,2}(\mathbf{r}) = \int g_{1,2}(\mathbf{p})\exp\left\{i\frac{p\mathbf{r}}{\hbar}\right\}d\mathbf{r}. \tag{A7}$$

As one sees from Eqs. (A7) and (A4), the wave functions, Eq. (A5), may be rewritten in terms of the envelope functions as follows:

$$\Psi(\mathbf{r}) = \sum_{s=1,2} u_{s,0}(\mathbf{r})\psi_s(\mathbf{r}). \tag{A8}$$

Step 2. In order to find boundary conditions for the Dirac equation, we investigate Schrödinger equation (A1) [in which $\varphi_{s,\mathbf{p}}(\mathbf{r})$ is changed to $\Psi(\mathbf{r})$] with the following boundary conditions:

$$\begin{aligned}&\Psi(\mathbf{r}) = 0, \quad y = 0:\\ &\Psi(\mathbf{r}) = \varphi^{(gr,in)}_{s,\mathbf{p}_0}(\mathbf{r}), \quad y \to +\infty.\end{aligned} \tag{A9}$$

Here $\varphi^{(gr,in)}_{s_0,\mathbf{p}_0}$ is the Bloch function incident to the boundary; this function is presented in Eq. (A8) in which the envelope functions $\psi_s(\mathbf{r})$ are solutions of Eq. (A6) at $V(\mathbf{r}) = 0$ and $\mathbf{p}_0 = (p_x, p_y^{(in)})$ where p_x is the conserving momentum projection on the edge and $p_y^{(in)} = -\sqrt{(\varepsilon/v)^2 - p_x^2}$.

To solve the problem of reflection by the abrupt edge at $y = 0$, the Green's function for Schrödinger equation (A1) is

used:

$$\left(-\frac{\hbar^2}{2m}\frac{\partial^2}{\partial \mathbf{r}^2}+U(\mathbf{r})-\varepsilon\right)G(\mathbf{r},\mathbf{r}')=\delta(\mathbf{r}-\mathbf{r}') \quad \text{(A10)}$$

in which the lattice potential $U(\mathbf{r})$ covers the whole plane (x, y).

Expanding $G(\mathbf{r}, \mathbf{r}')$ in the series of Bloch wave functions and using Eq. (A10) one finds

$$G(\mathbf{r},\mathbf{r}')=\sum_{s=1,2}\int\frac{\varphi^{(gr)\star}_{s,\mathbf{p}}(\mathbf{r})\varphi^{(gr)}_{s,\mathbf{p}}(\mathbf{r}')}{\varepsilon-\varepsilon^{(gr)}_s(\mathbf{p})+i\delta}d\mathbf{p} + \sum_{s\neq 1,2}\int\frac{\varphi^{\star}_{s,\mathbf{p}}(\mathbf{r})\varphi_{s,\mathbf{p}}(\mathbf{r}')}{\varepsilon-\varepsilon_s(\mathbf{p})+i\delta}d\mathbf{p}, \quad \text{(A11)}$$

where the summation goes over all energy bands while $\varepsilon^{(gr)}_s(\mathbf{p})=\pm vp$ is the graphene dispersion and $\delta\to+0$.

Taking into account the analytical properties of the virtual and graphene energy bands as functions of complex momenta and using Eqs. (A1), (A9), and (A11) together with Eq. (A8) we find that at $y \gg a$ (here a is the characteristic value of the period of the lattice) the wave function is the difference between the incident and outgoing Bloch functions of the infinite sample:

$$\Psi_{p_x}(\mathbf{r})=C\left(\varphi^{(gr)}_{s;p_x,p_y^{(in)}}(\mathbf{r})-\varphi^{(gr)}_{s;p_x,p_y(out)}(\mathbf{r})\right), \quad \text{(A12)}$$

where $p_y^{(in)}$ and $p_y^{(out)}=-p_y^{(in)}$ are the y projections of the quasiparticle momentum while C is the normalizing constant (details of calculations are given in Ref. [32]).

From Eqs. (A12) and (A8) one easily finds that at the distances from the lattice sharp edge much larger than the atomic spacing, $l \gg a$, the envelope function $\check{\Psi}(\mathbf{r})$ is the difference between the incident and outgoing wave functions [which are two independent solutions of the Dirac equation (A6)]:

$$\check{\Psi}(\mathbf{r})=e^{ixp_x}\left[e^{iyp_y^{(in)}}\begin{pmatrix}1\\ e^{i\varphi}\end{pmatrix}-e^{-i(yp_y^{(in)})}\begin{pmatrix}1\\ e^{-i\varphi}\end{pmatrix}\right], \quad \text{(A13)}$$

where the phase $\varphi=\arctan(p_y^{(in)}/p_x)$.

[1] D. Bohm, Phys. Rev. **75**, 502 (1949).
[2] J. Schmalian, Mod. Phys. Lett. B **24**, 2679 (2010).
[3] Y. Ohashi and T. Momoi, J. Phys. Soc. Jpn. **65**, 3254 (1996).
[4] C. X. Zhang and M. A. Zubkov, Phys. Rev. D **100**, 116021 (2019).
[5] H. Watanabe, J. Stat. Phys. **177**, 717 (2019).
[6] S. Bachmann and M. Fraas, Rev. Math. Phys. **33**, 2060011 (2021).
[7] A. Vilenkin, Phys. Rev. D **22**, 3080 (1980).
[8] H. Nielsen and M. Ninomiya, Phys. Lett. B **130**, 389 (1983).
[9] A. Y. Alekseev, V. V. Cheianov, and J. Fröhlich, Phys. Rev. Lett. **81**, 3503 (1998).
[10] K. Fukushima, D. E. Kharzeev, and H. J. Warringa, Phys. Rev. D **78**, 074033 (2008).
[11] A. Vilenkin, Phys. Rev. D **20**, 1807 (1979).
[12] D. T. Son and P. Surówka, Phys. Rev. Lett. **103**, 191601 (2009).
[13] K. Landsteiner, E. Megías, and F. Pena-Benitez, Phys. Rev. Lett. **107**, 021601 (2011).
[14] N. Yamamoto, Phys. Rev. D **92**, 085011 (2015).
[15] D. V. Else and T. Senthil, Phys. Rev. B **104**, 205132 (2021).
[16] H. Watanabe, Phys. Rev. Res. **4**, 013043 (2022).
[17] B.-L. Huang, M.-C. Chang, and C.-Y. Mou, J. Phys.: Condens. Matter **24**, 245304 (2012).
[18] D. Sticlet, B. Dóra, and J. Cayssol, Phys. Rev. B **88**, 205401 (2013).
[19] Y. Tada, Phys. Rev. B **92**, 104502 (2015).
[20] G.-Q. Zha, Z.-L. Yang, Y.-Y. Jin, and S.-P. Zhou, Phys. Rev. B **94**, 094510 (2016).
[21] N. Miyawaki and S. Higashitani, Phys. Rev. B **98**, 134516 (2018).
[22] J. Mannhart and D. Braak, J. Supercond. Novel Magn. **32**, 17 (2019).
[23] H. Kobayashi and H. Watanabe, Phys. Rev. Lett. **129**, 176601 (2022).
[24] W. J. Chetcuti, T. Haug, L.-C. Kwek, and L. Amico, SciPost Phys. **12**, 033 (2022).
[25] D. Kong, J. C. Randel, H. Peng, J. J. Cha, S. Meister, K. Lai, Y. Chen, Z.-X. Shen, H. C. Manoharan, and Y. Cui, Nano Lett. **10**, 329 (2010).
[26] J. J. Cha, J. R. Williams, D. Kong, S. Meister, H. Peng, A. J. Bestwick, P. Gallagher, D. Goldhaber-Gordon, and Y. Cui, Nano Lett. **10**, 1076 (2010).
[27] Y. Zou, Z.-G. Chen, Y. Huang, L. Yang, J. Drennan, and J. Zou, J. Phys. Chem. C **118**, 20620 (2014).
[28] L. A. Jauregui, M. T. Pettes, L. P. Rokhinson, L. Shi, and Y. P. Chen, Sci. Rep. **5**, 8452 (2015).
[29] C. Parra, T. H. Rodrigues da Cunha, A. W. Contryman, D. Kong, F. Montero-Silva, P. H. Rezende Gonçalves, D. D. Dos Reis, P. Giraldo-Gallo, R. Segura, F. Olivares, F. Niestemski, Y. Cui, R. Magalhaes-Paniago, and H. C. Manoharan, Nano Lett. **17**, 97 (2017).
[30] W. J. Liu, P. and J. Cha, Nat. Rev. Mater. **4**, 479 (2019).
[31] C. W. J. Beenakker, Rev. Mod. Phys. **80**, 1337 (2008).
[32] A. Kadigrobov, Low Temp. Phys. **44**, 1245 (2018).
[33] J. M. Luttinger and W. Kohn, Phys. Rev. **97**, 869 (1955).
[34] A. A. Slutskin, Zh. Eksp. Teor. Fiz. **58**, 1098 (1970) [Sov. Phys.-JETP **31**, 589 (1970)].
[35] M. Büttiker, Y. Imry, and R. Landauer, Phys. Lett. A **96**, 365 (1983).
[36] C.-K. Chan, N. H. Lindner, G. Refael, and P. A. Lee, Phys. Rev. B **95**, 041104(R) (2017).
[37] J. W. McIver, D. Hsieh, H. Steinberg, P. Jarillo-Herrero, and N. Gedik, Nat. Nanotechnol. **7**, 96 (2012).
[38] K. Kuroda, J. Reimann, J. Güdde, and U. Höfer, Phys. Rev. Lett. **116**, 076801 (2016).
[39] B. B. Kadomtsev, Sov. Phys. Usp. **11**, 328 (1968).